Lithium Treatment Prevents Neurocognitive Deficit Resulting from Cranial Irradiation

Eugenia M. Yazlovitskaya,[1,2] Eric Edwards,[1] Dinesh Thotala,[1] Allie Fu,[1] Kate L. Osusky,[1] William O. Whetsell, Jr.,[3] Braden Boone,[4] Eric T. Shinohara,[1] and Dennis E. Hallahan[1,2]

[1]Department of Radiation Oncology, [2]Vanderbilt-Ingram Cancer Center, [3]Department of Pathology, and [4]Vanderbilt Microarray Shared Resource, Vanderbilt University School of Medicine, Nashville, Tennessee

Abstract

Curative cancer treatment regimens often require cranial irradiation, resulting in lifelong neurocognitive deficiency in cancer survivors. This deficiency is in part related to radiation-induced apoptosis and decreased neurogenesis in the subgranular zone of the hippocampus. We show that lithium treatment protects irradiated hippocampal neurons from apoptosis and improves cognitive performance of irradiated mice. The molecular mechanism of this effect is mediated through multiple pathways, including Akt/glycogen synthase kinase-3β (GSK-3β) and Bcl-2/Bax. Lithium treatment of the cultured mouse hippocampal neurons HT-22 induced activation of Akt (1.5-fold), inhibition of GSK-3β (2.2-fold), and an increase in Bcl-2 protein expression (2-fold). These effects were sustained when cells were treated with lithium in combination with ionizing radiation. In addition, this combined treatment led to decreased expression (40%) of the apoptotic protein Bax. The additional genes regulated by lithium were identified by microarray, such as *decorin* and *Birc1f*. In summary, we propose lithium treatment as a novel therapy for prevention of deleterious neurocognitive consequences of cranial irradiation. (Cancer Res 2006; 66(23): 11179-86)

Introduction

Neuropathology resulting from cranial irradiation is rapidly becoming a common cause of neurocognitive deficits in adult and childhood cancer survivors. Cranial irradiation therapy is currently used for the treatment of both primary and metastatic brain tumors as well as leukemia and lymphoma involving the central nervous system. Detrimental consequences of cranial irradiation include long-term cognitive defects, especially in young children (1–4), which persist into adulthood (5). Evidence suggests that the pathogenesis of radiation-induced neurocognitive deficit may involve radiation-induced injury to proliferating neuronal progenitor cells in the subgranular zone of the hippocampus, which is a critical neurologic center for learning and memory (6). Relatively small doses of radiation have been shown to cause apoptosis in the subgranular zone of young rats and mice as shown by cellular morphology, terminal deoxynucleotidyl transferase–mediated dUTP nick end labeling (TUNEL) staining, and DNA laddering (7–10). Conversely, little to no apoptosis is observed in other areas of the cerebrum (9). Radiation also causes sharp and prolonged decline in neurogenesis in the subgranular zone (7, 8, 11–13). Clinical studies suggest that radiation-induced damage to the hippocampus plays a significant role in cognitive decline. Cognitive deficits observed in patients after cranial irradiation are related to hippocampal injury, such as learning, memory, and spatial processing (14, 15). Furthermore, radiation to the hippocampus is associated with more pronounced cognitive deficits (16).

Although no pharmacologic prophylaxis has been developed to attenuate radiation-induced neurocognitive deficits, several recent studies have shown that lithium exhibits neuroprotective effect against a variety of neurologic injuries (17–20). Lithium is a neuroprotective agent with known antiapoptotic activities, which is widely used in the treatment of bipolar mood disorder (21). Lithium also has a potential use for a wide range of neurodegenerative insults (22), including potassium and sodium deprivation (23), ceramide-induced apoptosis (24), and radiation (25). The neuroprotective effects of lithium require pretreatment, as the protection becomes apparent only after treatment for more than 2 to 3 days, and maximal effect is observed after 6 to 7 days of treatment. Pretreatment of neurons with lithium chloride (LiCl) for 7 days results in dose-dependent protection against glutamate-induced apoptosis with a EC_{50} value of ~1.3 mmol/L and maximal protection at 3 mmol/L (20). In rats subjected to left middle cerebral artery occlusion, a 16-day pretreatment with LiCl significantly reduces neurologic deficits and markedly decreases the size of brain damage (up to 56%; ref. 19). This neuroprotection occurs at therapeutic concentrations of LiCl. Specifically, significant protection occurs at 50 mg/kg LiCl with an almost maximal effect at 100 mg/kg.

The molecular mechanisms of lithium protection involve activation of antiapoptotic cell signaling pathway phosphatidylinositol 3-kinase/Akt, leading to the inhibition of glycogen synthase kinase-3β (GSK-3β; refs. 26, 27). Lithium causes inhibition of GSK-3β, acting both by displacing magnesium and indirectly inhibiting an activating phosphatase (27). GSK-3β has been shown to inhibit several critical transcription factors that promote cell survival and proliferation, including heat shock factor-1 (HSF-1), activator protein-1 (AP-1), Myc, nuclear factor-κB, nuclear factor of activated T cells, and cyclic AMP-responsive element binding protein (CREB; ref. 28). Lithium has also been shown to decrease levels of the proapoptotic proteins p53 and Bax while increasing levels of the prosurvival protein Bcl-2 (29). In the present study, we investigated LiCl as a potential neuroprotective agent against radiation-induced apoptosis. We analyzed the changes in gene and protein expression and activity following lithium administration before irradiating hippocampal neuronal cells as well as histologic and behavioral effects of lithium in rodent models of radiation-induced neuropathology.

Note: Supplementary data for this article are available at Cancer Research Online (http://cancerres.aacrjournals.org/).

E.M. Yazlovitskaya and E. Edwards contributed equally to this work.

Requests for reprints: Dennis E. Hallahan, Department of Radiation Oncology, Vanderbilt University, 1301 22nd Avenue South, B-902 The Vanderbilt Clinic, Nashville, TN 37232-5671. Phone: 615-343-9244; Fax: 615-343-3075; E-mail: Dennis.Hallahan@vanderbilt.edu.

doi:10.1158/0008-5472.CAN-06-2740

Materials and Methods

Animal models and treatment. Timed pregnant C57/BL/6J mice were obtained from The Jackson Laboratory (Bar Harbor, ME). Timed pregnant Sprague-Dawley rats were obtained from Charles River Laboratories (Wilmington, MA). All animal studies were conducted with the approval of the Institutional Animal Care and Use Committees and kept in a temperature and light-controlled environment with a 12-hour light/12-hour dark cycle. LiCl (Sigma, St. Louis, MO) was dissolved in PBS and gave to animals (40 or 80 mg/kg) via i.p. injection daily for 7 days starting on postnatal day 7. Time of treatment and dose of LiCl were chosen based on published data (22, 30) and our pilot experiments. The control treatment group received i.p. 150 mmol/L NaCl, which is most similar to LiCl analogue. Animals were treated with a single dose of radiation on postnatal day 14. Before irradiation, Sprague-Dawley rats were anesthetized with ketamine and xylazine. Mice were anesthetized in a similar fashion or restrained in plastic tubing. Animals were exposed to cranial irradiation using a Therapax DXT 300 X-ray machine (Pantak, Inc., Branford, CT) delivering 2.04 Gy/min at 80 kVp. For histologic stainings, animals were irradiated with 1, 2, 3, 4, 5, 6, 7, 8, or 10 Gy; 10 hours after irradiation, animals were sacrificed by cervical dislocation under isoflurane anesthesia. For Morris water maze studies, the mice were irradiated with 7 Gy; 6 weeks later, the animals were tested.

Morris water maze studies. The apparatus used was a circular pool 92 cm in diameter filled to a depth of 25 cm with water (20°C). Mice could escape the water by finding a clear square platform, approximately 10 × 10 cm, hidden several millimeters beneath the water. The pool was located in a room with no windows. Many visual cues were present in the room. For the initial visible platform experiments, the platform was marked with a plainly visible black flag. For the hidden platform experiments, the flag was removed and the water was made cloudy with white paint. A video camera suspended above the pool captured the subject's movements (two frames per second). The camera was connected to a Macintosh computer running software custom designed for analysis of Morris water maze studies. For the visible platform experiments, the location of the platform as well as the start location of the mouse changed for each trial. For the hidden platform experiment, the platform location remained constant for all trials, but the start locations changed with each trial. A trial started by placing a mouse into the water facing the wall of the pool in one of four possible start locations, and the camera was immediately activated. Each mouse was given up to 60 seconds to locate the platform. The trial was stopped when 60 seconds had expired or the mouse remained on the platform for >1 second. Four trials per day per mouse were done. All mice underwent the first trial of the day before undergoing a second trial. The visible platform trials were conducted for 5 days. The animals were given 2 days off before beginning the hidden platform experiments, which were conducted for a total of 9 days (5 days, 1 day off, 4 days). The average latency time (the length of time to find the platform in water) for each animal in each trial (±SE) was calculated. To achieve statistically significant results in the Morris water maze study, at least six male and six female mice per group (four groups) are required and each testing should be done on the same day. To minimize amount of tested animals and make process of testing feasible, one radiation dose of 7 Gy was used for this study. This dose was chosen as optimal for induction of apoptosis according to our histologic staining.

Brain sections and histologic stainings. To determine the numbers of apoptotic cells in the hippocampus, animals were sacrificed 10 or 24 hours after exposure to cranial radiation. The brain was removed and placed in 4% paraformaldehyde solution for 2 days. The frontal lobes were removed before embedding in paraffin. Fixed brains were cut coronally at the parieto-occipital junction, providing elongated exposure of each hippocampus. Coronal sections (5 μm) were then taken and placed on Superfrost Gold Plus slides (Erie Scientific, Portsmouth, NH). The sections were stained with H&E in the standard fashion. TUNEL staining was done with the DeadEnd Colorimetric TUNEL System (Promega, Madison, WI) following the manufacturer's instructions. The superior curvature of the hippocampus was used for quantification of apoptosis in all cases. The subgranular zone was identified as a two- to three-cell-wide layer adjacent to the granule cell layer, facing the hilus. TUNEL-positive or pyknotic cells were counted under a light microscope (×400). At least four fields were counted per animal, and at least three animals were used in experimental group. The average amount of pyknotic or TUNEL-positive cells (±SE) was calculated.

Cell cultures and treatment. Mouse hippocampal neuronal cells HT-22 were obtained from David Schubert (The Salk Institute, La Jolla, CA) and maintained in DMEM with 10% fetal bovine serum (FBS) and 1% penicillin/streptomycin (Life Technologies, Gaithersburg, MD). Human glioma D54 and mouse glioma GL261 cell lines were obtained from Dr. Yancie Gillespie (University of Alabama-Birmingham, Birmingham, AL) and maintained in DMEM with Nutrient Mixture F-12 1:1, 10% FBS, 1% sodium pyruvate, and 1% penicillin/streptomycin (Life Technologies). All cells were grown in a 5% CO_2 incubator at 37°C. LiCl was dissolved in the growth medium. Cells were treated with 3 mmol/L LiCl for 7 days before irradiation. Time of pretreatment and dose of LiCl were chosen based on published data (20, 22) and our pilot experiments. The control group received i.p. 150 mmol/L NaCl, which is most similar to LiCl. For the radiation of cells, a Mark I ^{137}Cs irradiator (J.L. Shepherd and Associates, San Fernando, CA) was used delivering 1.84 Gy/min. Turntable assured that the radiation was equally distributed.

Clonogenic survival. HT-22, GL261, and D54 cells were pretreated with 3 mmol/L LiCl for 7 days, counted with hemocytometer, plated on new plates, and allowed to attach for 5 hours. Cells were than irradiated with 0, 2, 4, 6, or 8 Gy. Medium was changed after irradiation. After 10 to 14 days, plates were fixed with 70% ethanol and stained with 1% methylene blue. Colonies over 50 cells were counted. Survival fraction was calculated as (number of colonies / number of cells plated) / (number of colonies for corresponding control / number of cells plated).

Apoptosis assays for cultured cells. HT-22 cells were pretreated with LiCl (3 mmol/L) for 7 days before irradiation. Camptothecin (5 μmol/L) was added to the cells 6 hours before harvest as a positive control for apoptosis. Pretreated cells were irradiated with 3 Gy and harvested 24 hours after irradiation. Annexin V-FITC Apoptosis Detection kit (BD PharMingen, San Diego, CA) was used for staining of apoptotic cells. Briefly, Annexin V-FITC (5 ng) and propidium iodide (50 ng) were added to 10^5 cells. Stained cells were analyzed by flow cytometry. For each treatment, the average fold increase of apoptotic cells over control (±SE) was calculated.

In separate experiments, morphologic assessment of apoptosis was done on HT-22 cells stained with 4′,6-diamidino-2-phenylindole (DAPI; Life Technologies). Cells were pretreated with 3 mmol/L LiCl for 7 days, irradiated with 3 Gy, and collected after 8, 16, and 24 hours. Apoptotic cells were identified by the presence of nuclear condensation and fragmentation. Apoptotic and nonapoptotic cells were counted in multiple randomly selected microscopic fields. The average percentage of apoptotic cells (±SE) was calculated.

Western immunoblotting. Total protein extraction from treated HT-22 cells was done using Mammalian Protein Extraction Reagent kit (Pierce, Rockford, IL). Protein concentration was quantified using bicinchoninic acid reagent (Pierce). Protein extracts (40 μg) were subjected to Western immunoblot analysis using antibodies for the detection of phosphorylated GSK-3β^{ser^9} and GSK-3$\beta^{Tyr^{216}}$, GSK-3β, phosphorylated Akt$^{ser^{473}}$, Akt, β-catenin, cyclin D1 (all from Cell Signaling Technology, Danvers, MA); NAIP (P-19), Bax (B-9), Bcl-2 (N-19; Santa Cruz Biotechnology, Santa Cruz, CA); and decorin (R&D Systems, Inc., Minneapolis, MN). Antibody to actin (Sigma) was used to evaluate protein loading in each lane. Immunoblots were developed using the Western Lightning Chemiluminescence Plus Detection System (Perkin-Elmer, Wellesley, MA) according to the manufacturer's protocol. Relative protein levels were determined by densitometry, normalized to actin, and calculated as the ratio of treated samples to untreated samples at each time point.

Microarray analysis of HT-22 cells. Total RNA (30-50 μg) was isolated from treated (3 mmol/L LiCl for 7 day) and control HT-22 cells using RNeasy Mini kit (Qiagen, Valencia, CA) and RNase-Free DNase Set (Qiagen). Microarray services were done by the Vanderbilt Microarray Shared

Resource (VMSR).[5] The RNA samples of high integrity were used to generate cDNA targets for hybridization to spotted arrays according to VMSR standard protocol.[5] Generated cDNA targets were purified using the QIAquick PCR purification kit (Qiagen), dried, and then differentially coupled to ester-linked Cy3 (controls) or Cy5 (LiCl treated) dye (Amersham, Piscataway, NJ). Cy3- and Cy5-labeled cDNA target pairs were combined, cleaned up over QIAquick columns (Qiagen), and hybridized for 16 hours at 42°C on microarrays containing all oligonucleotides from the Mouse Exonic Evidence Based Oligonucleotide (MEEBO) mouse genome set[6] using Maui Hyb Station (four-chamber model; BioMicro Systems, Inc., Salt Lake City, UT). MEEBO microarrays were produced by Microarrays, Inc. (Nashville, TN). The microarrays were washed, dried, and immediately scanned using a GenePix 4000B microarray scanner (Axon Instruments, Foster City, CA). Data were acquired by using GenePix Pro-6 software (Axon Instruments) and then analyzed using GeneSpring 7.1 software (Stratagene, La Jolla, CA). The Excel file was created for genes representing proteins with specific molecular functions (e.g., transcriptional factors) or known to be involved in different cellular processes (e.g., apoptosis).

Microarray experimental details are available for public review at ArrayExpress[7] with accession number E-MEXP-521.

Reverse transcription reactions for real-time PCR. For each sample, three basic reverse transcription reactions with 1 μg of starting RNA and SuperScript II Reverse Transcriptase (Invitrogen, Carlsbad, CA) were done according to the manufacturer's instructions. The reactions were purified using PCR Purification kit (Qiagen) and quantitated by spectrophotometry.

Real-time PCR using 384-well plates (relative quantification). Reverse-transcribed samples (25 ng/μL) were diluted with water (15% overage) to allow for 10 to 100 ng of template per well. Taqman FAM-labeled 20× probes were diluted with 2× Taqman Universal PCR Master Mix to 15% overage (Applied Biosystems, Foster City, CA). Four replicates were run for each sample/probe pair. Template loading and addition of Master Mix were done by the Multiprobe II HT EX liquid handling robot (Perkin-Elmer, Boston, MA). Cycling, data collection, and calculation of the relative quantity of probed RNA were done using the ABI Prism 7900 HT instrument (Applied Biosystems). The assays were done for the following mouse genes: *baculoviral inhibitor of apoptosis (IAP) repeat-containing 1f* (*Birc1f*), *decorin*, and *β-glucuronidase* as endogenous control.

Statistical analyses. The mean and SE of each treatment group were calculated for all experiments with statistical analysis. The number of samples is indicated in the description of each experiment. All statistical tests were two sided. $P < 0.05$ was considered statistically significant.

In Morris water maze studies, logarithmic transformation was applied to normalize the data first because of the skewed distribution of latency. To adjust the intracorrelation effect for mice that had multiple measurements, a restricted/residual maximum likelihood–based mixed-effect model was used for the analysis of latency variable. The mixed-effect model defines latency as a function of treatment group, gender, and time effects. Statistical Analysis System version 9.1 (SAS Institute, Inc., Cary, NC) was used for the analyses.

In all other experiments, variance was analyzed by Student's *t* test.

Results

Protective effect of lithium administration on radiation-induced cognitive deficit. Cranial irradiation in newborn rodents is associated with severe spatial navigation deficits in the Morris water maze (31) as well as other measures of cognitive function (32). These deficits can be accounted for neuronal precursor cell dysfunction in the subgranular zone caused by radiation (11). Published data (22, 30) suggest that 7 days of lithium pretreatment with the dose of 40 to 80 mg/kg show the maximal protection from neurodegenerative insults. To determine whether lithium treatment attenuates deficits in cognitive functions caused by radiation, C57/BL6 mice were treated with daily i.p. injections of 40 mg/kg LiCl starting postnatal day 7 and irradiated with 7 Gy on postnatal day 14. This dose was chosen as optimal for induction of apoptosis according to our histologic results (Supplementary Figs. S2 and S3; Figs. 2 and 3). Six weeks later, the animals were subjected to Morris water maze testing. We observed that female mice were particularly debilitated by irradiation, taking an average of twice as long to locate the hidden platform on the last day of testing compared with their male littermates (28.1 versus 14.6 seconds; $P = 0.027$; Supplementary Fig. S1; Fig. 1*A*). This sex difference in radiation-induced neurocognitive dysfunction supports clinical findings that females are at increased risk for developing severe cognitive deficits compared with their male counterparts (4, 5, 33). Although all groups of mice achieved comparable latency times on each day of training, significantly lower latency times were observed after 9 days of learning in mice treated with lithium before radiation compared with animals treated with radiation alone ($P = 0.02$ for both males and females; Supplementary Fig. S1; Fig. 1*B*). The latency time was 28 seconds in irradiated females, which was reduced to 14 seconds in LiCl-pretreated female littermates ($P = 0.024$). Likewise, irradiated males showed latency time of 14 seconds, which was reduced to 7 seconds in LiCl-pretreated male littermates ($P = 0.037$).

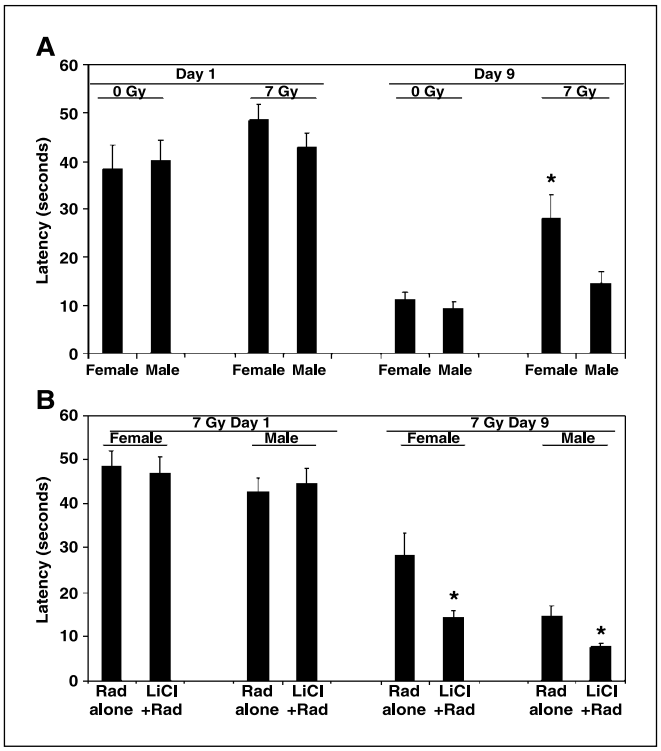

Figure 1. Improvement of cognitive function in mice treated with cranial irradiation due to lithium prophylaxis. Cognitive function following cranial irradiation was studied in C57/BL6 mice. One-week-old pups were treated with daily i.p. injections of LiCl (40 mg/kg) or PBS for 7 days. On the 7th day of LiCl treatment, the pups were treated with 7 Gy of cranial irradiation or sham irradiation. Six weeks later, the animals were studied using hidden Morris water maze testing. *Columns,* average latencies of (*A*) unirradiated versus irradiated male or female mice on days 1 and 9 and (*B*) irradiated versus irradiated after lithium treatment of male and female mice on days 1 and 9; *bars,* SE. *, $P < 0.05$, Student's *t* test.

[5] http://www.vmsr.net.
[6] http://mmc.ucsf.edu/Meebo.html.
[7] http://www.ebi.ac.uk/arrayexpress/query/entry.

Attenuation of radiation-induced apoptosis by LiCl in hippocampal subgranular zone neurons in rodent models. We determined effect of radiation dose on the level of apoptosis in the subgranular zone by exposing 2-week-old mice to various doses of cranial irradiation. Pyknotic nuclei were counted within the subgranular zone of control and irradiated mouse brains (Fig. 2*A*). A dose-dependent increase in subgranular zone neuronal apoptosis was observed (Fig. 2*B*). A dose as low as 2 Gy induced apoptosis in the neuronal precursor cells of the subgranular zone [70 per high-power field (HPF)]; 10 Gy resulted in 3-fold increase in apoptosis (200 per HPF; Fig. 2*B*). Similar results were obtained using TUNEL staining of brain sections from mice that were treated with 3 or 7 Gy (Supplementary Fig. S2A-B).

To determine whether lithium attenuates radiation-induced apoptosis in the subgranular zone, we started to treat mice pups with daily i.p. injections of LiCl beginning on postnatal day 14. On postnatal day 21, the animals were treated with cranial irradiation. Ten hours later, sections of the hippocampus were analyzed for apoptosis using TUNEL staining (Fig. 3*A*). Subgranular zone neurons of animals treated with 7 Gy showed 50-fold increase in TUNEL stain compared with mice that were sham irradiated (0 Gy) or treated with LiCl alone. LiCl administration for 7 days before irradiation resulted in a 2-fold decrease in apoptosis in subgranular zone neurons in the mice brain compared with brains treated with 7 Gy alone (P = 0.012; Fig. 3*B*). This protective effect of LiCl from radiation-induced apoptosis in hippocampus was additionally studied in different rodent model, Sprague-Dawley rat pups. In similar setting, we obtained similar results (Supplementary Fig. S3A-B). The radioprotective effect of lithium in hippocampal neurons is therefore observed in both animal models.

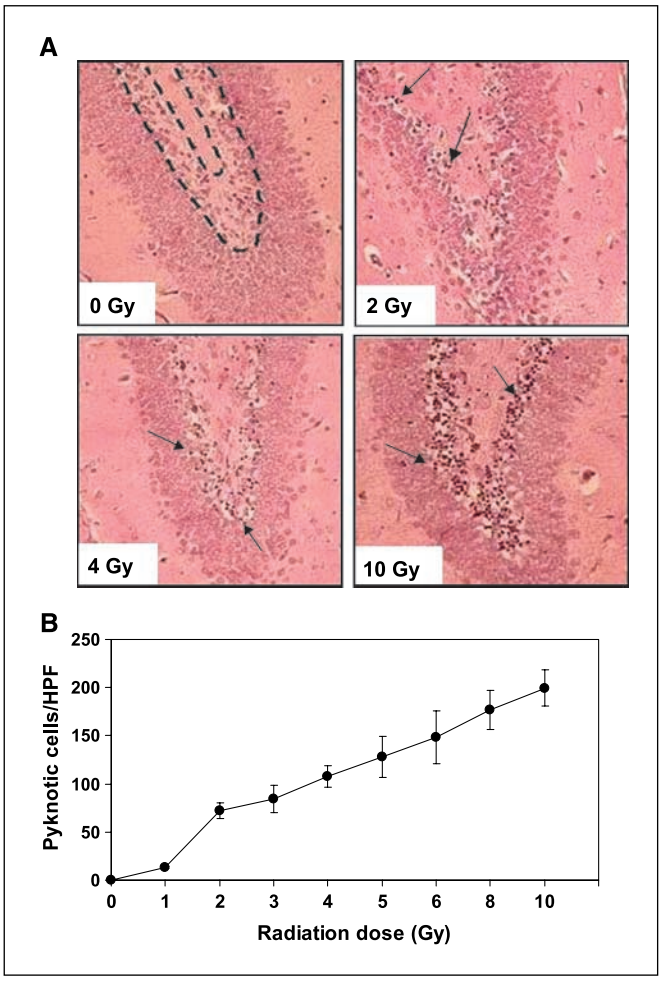

Figure 2. Radiation effects on hippocampal neurons in mouse brain. Two-week-old C57/BL6 mice were treated with the indicated doses of cranial irradiation. Ten hours later, the animals were sacrificed and brains were immediately fixed and coronally sectioned. Sections that contained hippocampus were stained with H&E. *A,* representative photographs (×200) of mouse hippocampus treated with 0, 2, 4, and 10 Gy. The subgranular zone is outlined in the 0 Gy frame. *Arrows,* examples of pyknotic cells. *B,* eight HPFs (×400) were observed and pyknotic cells were counted for each experimental group. *Points,* average number of pyknotic cells per HPF for each radiation dose group from three independent experiments; *bars,* SE.

LiCl effect on survival and apoptosis of irradiated HT-22, GL261, and D54 cells. Lithium is neuroprotective in several settings (17–20). A therapeutic advantage requires little protection of intracranial neoplasms, such as gliomas, which is concurrent with neuroprotection. To determine whether lithium pretreatment improved cell viability in irradiated hippocampal neurons compared with glioma cells, HT-22, GL261, and D54 cells were treated with 3 mmol/L LiCl for 7 days. Cells were irradiated, and survival was determined by clonogenic analysis. With increased dose of irradiation, LiCl treatment showed a selective increased viability of hippocampal neurons (Fig. 4*A*), whereas it had no effect on the survival of irradiated GL261 or D54 cancer cells (Fig. 4*B* and *C*). In apoptosis study, GL261 and D54 cells showed no radiation-induced apoptosis and therefore no effect of LiCl on apoptosis (data not shown). On the contrary, lithium protective effect in irradiated HT-22 cells, which we observed in clonogenic assay, was confirmed in apoptosis studies. Representative flow cytometry results following Annexin V-FITC and propidium iodide staining of HT-22 cells are shown in Fig. 5*A*. The apoptotic fraction of the cells in each treatment group was calculated as fold increase versus control group of three separate experiments (Fig. 5*B*). Twenty-four hours after irradiation with 3 Gy, apoptosis in HT-22 cells increased 9-fold compared with untreated control cells. However, cells pretreated with LiCl showed attenuated radiation-induced apoptosis, up to 3-fold versus 9-fold in cells treated with radiation alone (P = 0.005; Fig. 5*B*). The radioprotective effect of lithium in HT-22 cells was also assayed by using DAPI staining. Lithium produced up to a 4-fold decrease in apoptosis of LiCl-treated cells compared with cells treated with radiation alone (P = 0.011 for 8-hour time points, P = 0.015 for 16-hour time points, P = 0.031 for 24-hour time points; Fig. 5*C*).

Effect of LiCl on Akt/GSK-3β pathway and Bcl-2/Bax protein expression ratio in HT-22 cells. Lithium is a known inhibitor of GSK-3β (27, 34). To determine whether lithium treatment affects GSK-3β activity in hippocampal neurons and whether it is time dependent, total protein was extracted from HT-22 cells treated with LiCl for 1 to 5 days. Western immunoblotting with antibody specific for phosphorylated GSK-3β^{ser^9} is shown in Fig. 6*A*. Inhibitory phosphorylation of GSK-3β^{ser^9} was first observed after 3 days of treatment with 3 mmol/L LiCl (1.5-fold increase over time-matching control) and significantly increased after 5 days (2.2-fold increase), suggesting that 5 days of 3 mmol/L LiCl treatment are required to achieve inhibition of GSK-3β in HT-22 cells. This lithium-triggered inhibition of GSK-3β activity was sustained after irradiation of LiCl-treated HT-22 cells as shown by the increased inhibitory phosphorylation of GSK-3β^{ser^9} (2.2-fold increase) and by decreased activating phosphorylation of GSK-3$\beta^{Tyr^{216}}$ (40% decrease; Fig. 6*B*). This partially could be attributed to activation of Akt, the upstream kinase for negative regulation of

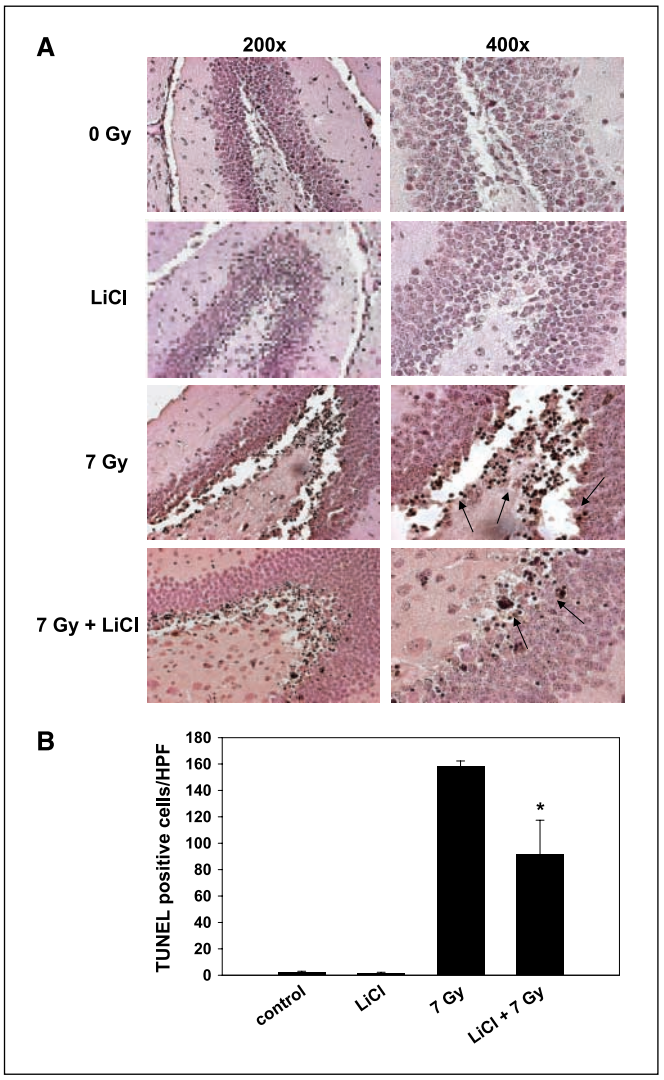

Figure 3. LiCl protection of hippocampal neurons from radiation-induced apoptosis *in vivo*. Two-week-old C57/BL/6J mice pups were treated with daily i.p. injections of LiCl (40 mg/kg) or PBS. On the 7th day of LiCl treatment, the pups were treated with 7 Gy of cranial irradiation or sham irradiation. Ten hours later, the animals were sacrificed and brains were fixed and coronally sectioned. TUNEL staining and hematoxylin counterstaining were done on sections that contained the hippocampus. *A,* representative photomicrographs of mouse hippocampus treated with 0 Gy, LiCl, 7 Gy, or 7 Gy + LiCl (HPF, ×200 and ×400). *Arrows,* examples of TUNEL-positive cells. *B, columns,* average numbers of TUNEL-positive cells per HPF in each treatment group from three independent experiments; *bars,* SE. *, $P < 0.05$, Student's *t* test.

GSK-3β activity. As compared with ionizing radiation, lithium induced higher level phosphorylation of $Akt^{ser^{473}}$ (1.5-fold versus 1.2-fold increase; Fig. 6*B*). In addition, lithium pretreatment altered radiation-induced response of the GSK-3β downstream targets: an increased protein accumulation was observed for β-catenin and cyclin D1 (2-fold increase for both proteins; Fig. 6*B*).

Bcl-2 is an antiapoptotic signaling molecule that inhibits the proapoptotic factor Bax through heterodimerization (35). Bax function is required for radiation-induced apoptosis in the hippocampus (36). Lithium has been shown to increase levels of Bcl-2 and decrease levels of Bax (29). In our study, HT-22 cultured hippocampal neurons treated with 3 mmol/L LiCl showed 2-fold increase in protein expression of Bcl-2, whereas expression of Bax was not affected (Fig. 6*A*). At 6 hours after irradiation with 3 Gy, protein level of Bcl-2 remained increased in LiCl-treated HT-22 cells (1.7-fold increase). In the same cells, expression of Bax became decreased up to 40%, promoting an antiapoptotic cellular response (Fig. 6*B*).

LiCl-dependent regulation of multiple genes in HT-22 cells. To investigate neuroprotective effect of lithium on gene expression, we used microarray analysis approach. The expression of >30,000 mouse genes in HT-22 neuronal cells was analyzed after 7 days of treatment with 3 mmol/L LiCl compared with cells treated with PBS alone (Database S1). LiCl induced a >2-fold increase in several dozen genes involved in the antiapoptotic signaling, DNA repair mechanism, and neurogenesis or >2-fold reduction in expression of genes with proapoptotic activity (Database S1). We choose some of genes involved in apoptosis for further analysis. The results of

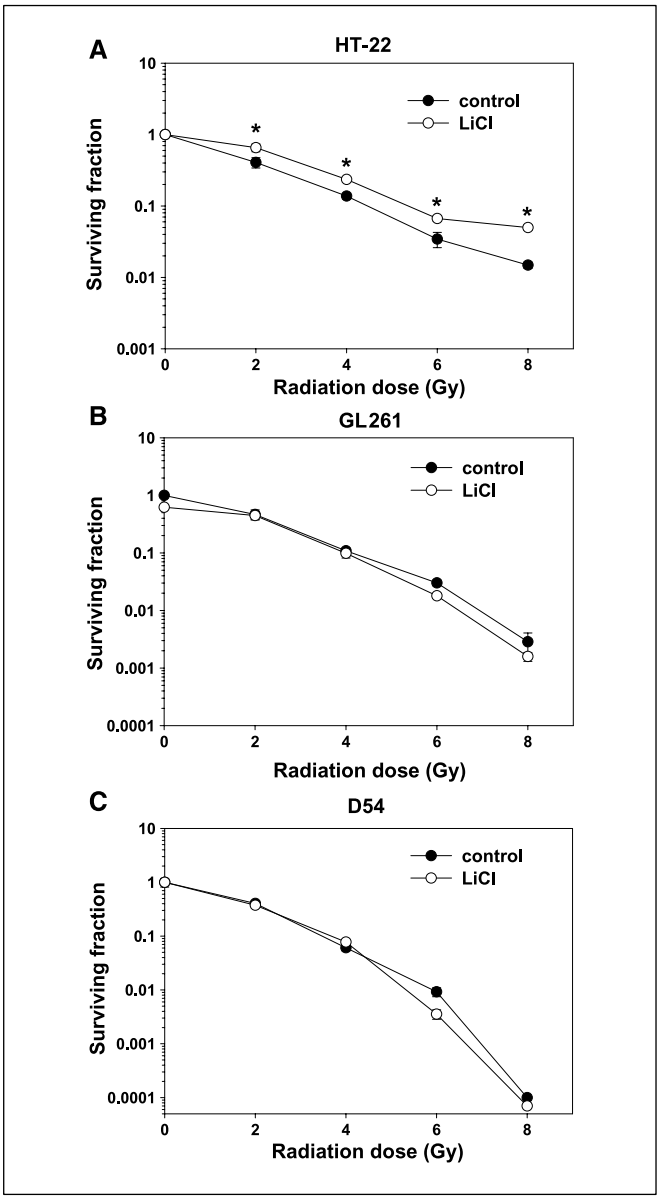

Figure 4. LiCl effect on viability of irradiated hippocampal neuronal HT-22 cells and glioma GL261 and D54 cells. HT-22 (*A*), GL261 (*B*), and D54 (*C*) cells were treated with 3 mmol/L LiCl for 7 days followed by irradiation with the indicated doses. *Points,* surviving fractions of cells treated with 7 days of lithium (○) or without lithium (●) in clonogenic assays; *bars,* SE.

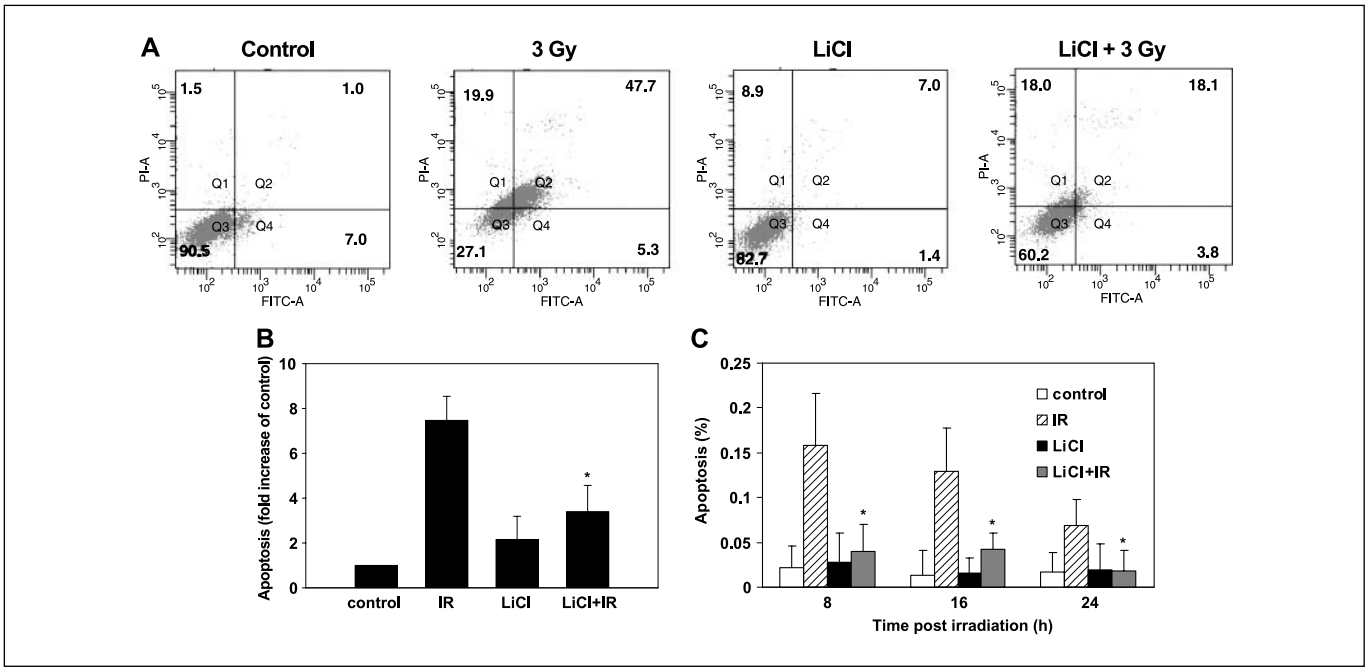

Figure 5. Attenuation of apoptosis in irradiated HT-22 hippocampal neuronal cells by LiCl treatment. Mouse hippocampal HT-22 neuronal cells were treated with 3 mmol/L LiCl for 7 days before irradiation with 3 Gy. *A* and *B,* cells were collected 24 hours after irradiation, stained with Annexin V-FITC and propidium iodide, and analyzed by flow cytometry. *A,* representative diagrams of distribution of stained cells (*quadrant 1,* necrosis; *quadrant 2*, late apoptosis/necrosis; *quadrant 3,* viable cells; *quadrant 4,* early apoptosis). *B, columns,* average fold increase of percentage apoptotic cells in each treatment normalized to control cells from three independent experiments; *bars,* SE. *, $P < 0.05$, Student's *t* test. *C,* morphologic analysis of apoptosis in irradiated HT-22 hippocampal neuronal cells was done under microscopy following DAPI staining. Apoptotic and nonapoptotic cells were counted in multiple randomly selected fields. *Columns,* amount of apoptotic cells as the percentage of total cells of three independent experiments; *bars,* SE. *, $P < 0.05$, Student's *t* test.

real-time PCR confirmed that LiCl treatment of HT-22 cells leads to preferential increased expression of antiapoptotic genes. For example, *decorin* and *Birc1f* showed increase in mRNA expression of LiCl-treated HT-22 cells, 2.5-fold and 1.4-fold, correspondingly. We also did Western blot analysis for decorin and NIAP in HT-22 cells treated with 3 mmol/L LiCl for 7 days before irradiation with 3 Gy. Compared with untreated cells, lithium treatment caused a significant increase of 1.6-fold in decorin protein expression (Fig. 6*C*). In both untreated and LiCl-treated cells, we detected full-length and several proteolytic fragments of NAIP (a member of BIRC family), which were reported previously (37). In addition, a LiCl-dependent elevation from 1.4-fold to 2.2-fold in all protein forms of NAIP occurred in these neuronal cells. Interestingly, the 60-kDa NAIP (a member of BIRC family) fragment showed the highest increase of 2.2-fold in response to lithium. In direct contrast, the 60-kDa fragment was substantially reduced following irradiation (33% decrease; 1.7-fold versus 2.2-fold; Fig. 6*C*), suggesting a potentially unique involvement of NAIP in lithium radioprotective effect for neurons.

Discussion

Cranial irradiation has been shown to cause significant long-term impairment in hippocampal-dependent learning and memory (31, 32). In our study, 7 Gy of irradiation in 2-week-old pups caused significant destruction of performance in the Morris water maze, which is associated with altered hippocampal function (11). This alteration could be due to hippocampus-specific apoptosis because in our study even small doses of radiation (1-2 Gy) induced apoptosis in the subgranular zone of the developing hippocampus but not in other areas of the brain. Female mice were more affected than males, which is also seen in clinical studies of females suffering more severe radiation-induced cognitive decline compared with males (4, 5, 33, 38). Treatment with LiCl before cranial irradiation improved performance in the Morris water maze, suggesting that lithium attenuates the cognitive deficits that result from cranial irradiation. Lithium is neuroprotective against a variety of cytotoxic processes, including serum starvation (17), oxygen and glucose deprivation (18, 19), glutamate-mediated excitotoxicity (20), and others (22, 27). Because impaired performance in the Morris water maze is an indication of altered hippocampal function (11) and lithium has also been shown to delay radiation-induced apoptosis in the external granule cells of newborn mouse cerebellum (25), we studied effect of LiCl on apoptosis in irradiated hippocampal neurons. We found that 7 days of pretreatment with 3 mmol/L LiCl significantly decreased radiation-induced apoptosis of hippocampal neurons in rodent models. To confirm antiapoptotic mechanism of lithium protection from radiation, we applied cell culture models. By using clonogenic and apoptosis assays, we found that LiCl treatment increased survival of irradiated hippocampal neurons in culture through inhibition of apoptosis but did not affect glioma cancer cell lines. This may be related to findings that cancer cells typically do not undergo apoptosis in response to ionizing radiation, in contrast to hippocampal neurons from the subgranular zone. We speculate that the protective effect of LiCl is mediated primarily through the inhibition of apoptosis, which is minimal in irradiated cancer cells. This differential response to radiation provides a means to improve the therapeutic effect of cranial irradiation.

There is some evidence to suggest that inhibition of proapoptotic GSK-3β pathway is in part a mechanism of lithium protection. Administration of antisense oligonucleotides of GSK-3β protected hippocampal cells in culture from β-amyloid toxicity (39). Lithium

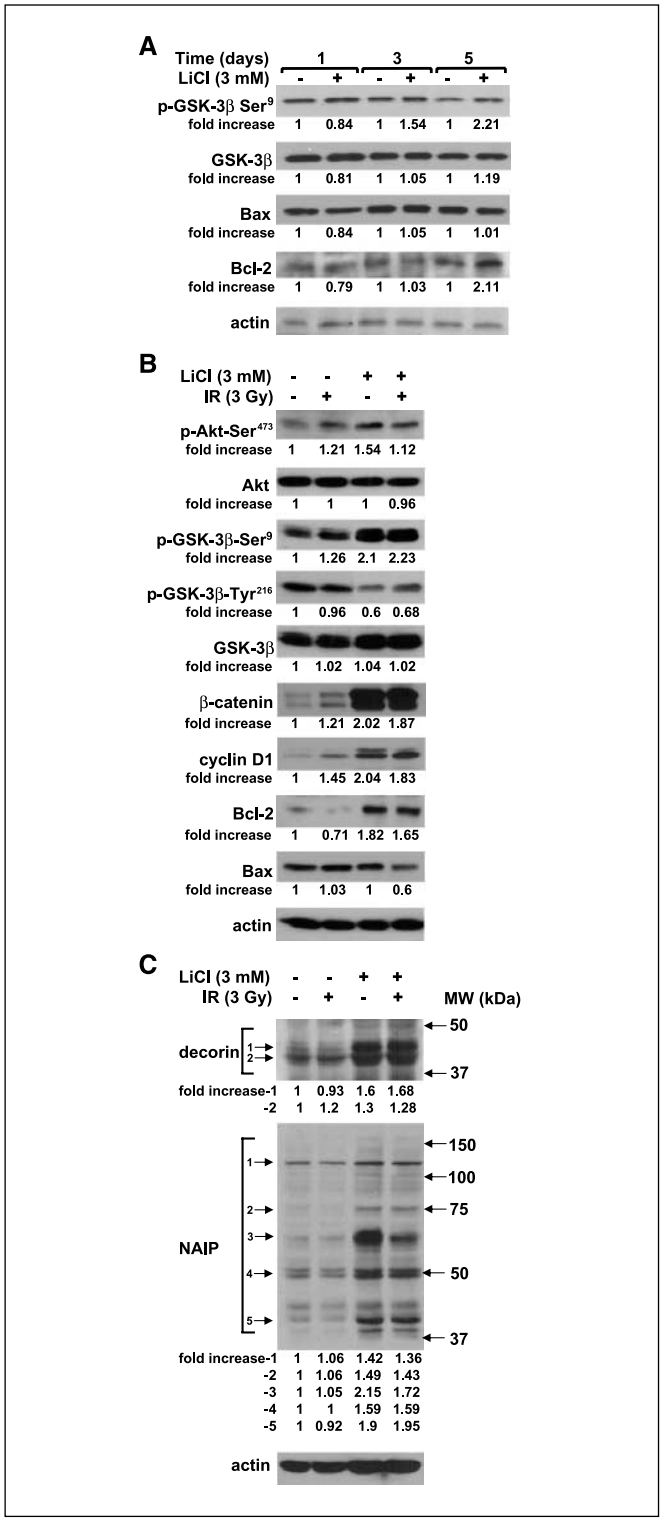

Figure 6. Effect of LiCl on Akt/GSK-3β pathway and Bcl-2/Bax protein expression in HT-22 neuronal cells. HT-22 mouse hippocampal neuronal cells were either (*A*) treated with 3 mmol/L LiCl for 1, 3, and 5 days or (*B-C*) pretreated with 3 mmol/L LiCl for 7 days, then irradiated with 3 Gy, and harvested 6 hours later. Cells were lysed and total protein was analyzed by Western blot analysis (40 μg protein/lane). Antibodies to phosphorylated GSK-3β (Ser^{9} and Tyr^{216}), GSK-3β, phosphorylated Akt (Ser^{473}), Akt, β-catenin, cyclin D1, Bax, Bcl-2, NAIP, and decorin were used to analyze levels of expression of these proteins. Actin was used to normalize protein loading in each lane. Relative protein levels were determined by densitometry and calculated as the ratio of treated samples to untreated samples at each time point.

and GSK-3β inhibitors have been shown to protect neuronal outgrowth (40, 41). Lithium inhibits GSK-3β activity both by displacing magnesium and indirectly inhibiting an activating phosphatases (27), which leads to accumulation of inactive form of phosphorylated GSK-3β^{ser9} (34). We found that 5 days of LiCl treatment increased levels of phosphorylated GSK-3β^{ser9}, which is consistent with prior studies (34). This lithium-triggered accumulation of inactive form of GSK-3β was sustained after irradiation. In addition, lithium pretreatment altered radiation-induced response of proteins, which are upstream and downstream of GSK-3β, including activation of Akt and protein accumulation of β-catenin and cyclin D1. GSK-3β-dependent phosphorylation of β-catenin (28) and cyclin D1 (42) promotes their ubiquitin-mediated proteolytic degradation, which is a necessary part of normal transcription process and cell cycle progression. Lithium-triggered inhibition of GSK-3β in HT-22 cells may cause stabilization and accumulation of β-catenin and cyclin D1, leading to alterations in cell cycle, and subsequent protection from radiation-induced apoptosis.

GSK-3β is known to inhibit several crucial transcription factors involved in cell survival and proliferation. These transcription factors include CREB (43), HSF-1 (44, 45), and AP-1 (46). Lithium also has been shown to decrease levels of p53 and Bax while increasing levels of Bcl-2, and 5 days of lithium treatment were required to achieve maximal effect on protein levels (29). In the present study, 5 days of LiCl treatment of HT-22 cells induced an increase in Bcl-2 but did not affect expression of Bax. However, combination of LiCl and radiation leads to sustained increased level of Bcl-2 and decreased level of Bax, creating classic anti-apoptotic expression ratio of Bcl-2 family proteins. This could be attributed to lithium-dependent inhibition of GSK-3β (29, 47). Taken together, the molecular mechanism of the radioprotective effect of lithium could be mediated in part by inhibition of GSK-3β.

In our study, 5 to 7 days of LiCl treatment were required to achieve protection from radiation effects. In contrast, 24 hours of treatment had no effect on neuronal cell viability (data not shown). This is consistent with the findings of Nonaka et al. (20), which show significant neuroprotection of cerebellar granule cells in culture only after prolonged lithium treatment. These findings can be explained by modulation of transcription of genes that regulate apoptosis, which is likely required for the neuroprotective effect of lithium. In our study of LiCl-treated hippocampal neurons, microarray analysis revealed set of genes, including proapoptotic and antiapoptotic, which levels of expression are regulated by lithium. Specifically, decorin and NAIP represent interesting novel molecular targets. Decorin is an important antiapoptotic factor in a variety of cell systems (48). NAIP belongs to BIRC proteins, also known as family of IAP proteins, which are antiapoptotic both *in vivo* and *in vitro* (49).

In summary, pretreatment of subjects with lithium before cranial irradiation preserves neurocognitive function and prevents deleterious consequences of radiation therapy. Lithium radioprotection offers novel therapeutic targets for enhanced protection of normal neuronal tissue during radiotherapy.

Acknowledgments

Received 7/24/2006; revised 9/7/2006; accepted 9/27/2006.

Grant support: NIH grants R01-CA112385, R01-CA88076, R01-CA89674, R01-CA89888, and P50-CA90949; Ingram Charitable Fund; and Vanderbilt-Ingram Cancer Center grant CCSG P30-CA68485.

The costs of publication of this article were defrayed in part by the payment of page charges. This article must therefore be hereby marked *advertisement* in accordance with 18 U.S.C. Section 1734 solely to indicate this fact.

References

1. Meadows AT, Gordon J, Massari DJ, Littman P, Fergusson J, Moss K. Declines in IQ scores and cognitive dysfunctions in children with acute lymphocytic leukaemia treated with cranial irradiation. Lancet 1981;2:1015–8.
2. Robison LL, Nesbit ME, Jr., Sather HN, Meadows AT, Ortega JA, Hammond GD. Factors associated with IQ scores in long-term survivors of childhood acute lymphoblastic leukemia. Am J Pediatr Hematol Oncol 1984;6:115–21.
3. Silverman CL, Palkes H, Talent B, Kovnar E, Clouse JW, Thomas PR. Late effects of radiotherapy on patients with cerebellar medulloblastoma. Cancer 1984;54:825–9.
4. Jannoun L, Bloom HJ. Long-term psychological effects in children treated for intracranial tumors. Int J Radiat Oncol Biol Phys 1990;18:747–53.
5. Pui CH, Cheng C, Leung W, et al. Extended follow-up of long-term survivors of childhood acute lymphoblastic leukemia. N Engl J Med 2003;349:640–9.
6. Deweer B, Pillon B, Pochon JB, Dubois B. Is the HM story only a "remote memory"? Some facts about hippocampus and memory in humans. Behav Brain Res 2001;127:209–24.
7. Mizumatsu S, Monje ML, Morhardt DR, Rola R, Palmer TD, Fike JR. Extreme sensitivity of adult neurogenesis to low doses of X-irradiation. Cancer Res 2003;63:4021–7.
8. Peissner W, Kocher M, Treuer H, Gillardon F. Ionizing radiation-induced apoptosis of proliferating stem cells in the dentate gyrus of the adult rat hippocampus. Brain Res Mol Brain Res 1999;71:61–8.
9. Nagai R, Tsunoda S, Hori Y, Asada H. Selective vulnerability to radiation in the hippocampal dentate granule cells. Surg Neurol 2000;53:503–6; discussion 506–7.
10. Ferrer I, Serrano T, Alcantara S, Tortosa A, Graus F. X-ray-induced cell death in the developing hippocampal complex involves neurons and requires protein synthesis. J Neuropathol Exp Neurol 1993;52:370–8.
11. Monje ML, Mizumatsu S, Fike JR, Palmer TD. Irradiation induces neural precursor-cell dysfunction. Nat Med 2002;8:955–62.
12. Madsen TM, Kristjansen PE, Bolwig TG, Wortwein G. Arrested neuronal proliferation and impaired hippocampal function following fractionated brain irradiation in the adult rat. Neuroscience 2003;119:635–42.
13. Tada E, Parent JM, Lowenstein DH, Fike JR. X-irradiation causes a prolonged reduction in cell proliferation in the dentate gyrus of adult rats. Neuroscience 2000;99:33–41.
14. Abayomi OK. Pathogenesis of irradiation-induced cognitive dysfunction. Acta Oncol 1996;35:659–63.
15. Roman DD, Sperduto PW. Neuropsychological effects of cranial radiation: current knowledge and future directions. Int J Radiat Oncol Biol Phys 1995;31:983–98.
16. Abayomi OK. Pathogenesis of cognitive decline following therapeutic irradiation for head and neck tumors. Acta Oncol 2002;41:346–51.
17. Hongisto V, Smeds N, Brecht S, Herdegen T, Courtney MJ, Coffey ET. Lithium blocks the c-Jun stress response and protects neurons via its action on glycogen synthase kinase 3. Mol Cell Biol 2003;23:6027–36.
18. Cimarosti H, Rodnight R, Tavares A, et al. An investigation of the neuroprotective effect of lithium in organotypic slice cultures of rat hippocampus exposed to oxygen and glucose deprivation. Neurosci Lett 2001;315:33–6.
19. Nonaka S, Chuang DM. Neuroprotective effects of chronic lithium on focal cerebral ischemia in rats. Neuroreport 1998;9:2081–4.
20. Nonaka S, Hough CJ, Chuang DM. Chronic lithium treatment robustly protects neurons in the central nervous system against excitotoxicity by inhibiting *N*-methyl-D-aspartate receptor-mediated calcium influx. Proc Natl Acad Sci U S A 1998;95:2642–7.
21. Jope RS. Anti-bipolar therapy: mechanism of action of lithium. Mol Psychiatry 1999;4:117–28.
22. Chuang DM, Chen RW, Chalecka-Franaszek E, et al. Neuroprotective effects of lithium in cultured cells and animal models of diseases. Bipolar Disord 2002;4:129–36.
23. Nonaka S, Katsube N, Chuang DM. Lithium protects rat cerebellar granule cells against apoptosis induced by anticonvulsants, phenytoin, and carbamazepine. J Pharmacol Exp Ther 1998;286:539–47.
24. Centeno F, Mora A, Fuentes JM, Soler G, Claro E. Partial lithium-associated protection against apoptosis induced by C2-ceramide in cerebellar granule neurons. Neuroreport 1998;9:4199–203.
25. Inouye M, Yamamura H, Nakano A. Lithium delays the radiation-induced apoptotic process in external granule cells of mouse cerebellum. J Radiat Res (Tokyo) 1995;36:203–8.
26. Klein PS, Melton DA. A molecular mechanism for the effect of lithium on development. Proc Natl Acad Sci U S A 1996;93:8455–9.
27. Jope RS. Lithium and GSK-3: one inhibitor, two inhibitory actions, multiple outcomes. Trends Pharmacol Sci 2003;24:441–3.
28. Grimes CA, Jope RS. The multifaceted roles of glycogen synthase kinase 3β in cellular signaling. Prog Neurobiol 2001;65:391–426.
29. Chen RW, Chuang DM. Long term lithium treatment suppresses p53 and Bax expression but increases Bcl-2 expression. A prominent role in neuroprotection against excitotoxicity. J Biol Chem 1999;274:6039–42.
30. Dou H, Ellison B, Bradley J, et al. Neuroprotective mechanisms of lithium in murine human immunodeficiency virus-1 encephalitis. J Neurosci 2005;25:8375–85.
31. Czurko A, Czeh B, Seress L, Nadel L, Bures J. Severe spatial navigation deficit in the Morris water maze after single high dose of neonatal x-ray irradiation in the rat. Proc Natl Acad Sci U S A 1997;94:2766–71.
32. Rola R, Raber J, Rizk A, et al. Radiation-induced impairment of hippocampal neurogenesis is associated with cognitive deficits in young mice. Exp Neurol 2004;188:316–30.
33. Bleyer WA, Fallavollita J, Robison L, et al. Influence of age, sex, and concurrent intrathecal methotrexate therapy on intellectual function after cranial irradiation during childhood: a report from the Children's Cancer Study Group. Pediatr Hematol Oncol 1990;7:329–38.
34. De Sarno P, Li X, Jope RS. Regulation of Akt and glycogen synthase kinase-3β phosphorylation by sodium valproate and lithium. Neuropharmacology 2002;43:1158–64.
35. Yin XM, Oltvai ZN, Korsmeyer SJ. BH1 and BH2 domains of Bcl-2 are required for inhibition of apoptosis and heterodimerization with Bax. Nature 1994;369:321–3.
36. Chong MJ, Murray MR, Gosink EC, et al. Atm and Bax cooperate in ionizing radiation-induced apoptosis in the central nervous system. Proc Natl Acad Sci U S A 2000;97:889–94.
37. Hutchison JS, Derrane RE, Johnston DL, et al. Neuronal apoptosis inhibitory protein expression after traumatic brain injury in the mouse. J Neurotrauma 2001;18:1333–47.
38. Christie D, Leiper AD, Chessells JM, Vargha-Khadem F. Intellectual performance after presymptomatic cranial radiotherapy for leukaemia: effects of age and sex. Arch Dis Child 1995;73:136–40.
39. Takashima A, Noguchi K, Sato K, Hoshino T, Imahori K. Tau protein kinase I is essential for amyloid β-protein-induced neurotoxicity. Proc Natl Acad Sci U S A 1993;90:7789–93.
40. Jiang H, Guo W, Liang X, Rao Y. Both the establishment and the maintenance of neuronal polarity require active mechanisms: critical roles of GSK-3β and its upstream regulators. Cell 2005;120:123–35.
41. Yoshimura T, Kawano Y, Arimura N, Kawabata S, Kikuchi A, Kaibuchi K. GSK-3β regulates phosphorylation of CRMP-2 and neuronal polarity. Cell 2005;120:137–49.
42. Liang J, Slingerland JM. Multiple roles of the PI3K/PKB (Akt) pathway in cell cycle progression. Cell Cycle 2003;2:339–45.
43. Grimes CA, Jope RS. CREB DNA binding activity is inhibited by glycogen synthase kinase-3β and facilitated by lithium. J Neurochem 2001;78:1219–32.
44. Chu B, Soncin F, Price BD, Stevenson MA, Calderwood SK. Sequential phosphorylation by mitogen-activated protein kinase and glycogen synthase kinase 3 represses transcriptional activation by heat shock factor-1. J Biol Chem 1996;271:30847–57.
45. Bijur GN, Jope RS. Opposing actions of phosphatidylinositol 3-kinase and glycogen synthase kinase-3β in the regulation of HSF-1 activity. J Neurochem 2000;75:2401–8.
46. Boyle WJ, Smeal T, Defize LH, et al. Activation of protein kinase C decreases phosphorylation of c-Jun at sites that negatively regulate its DNA-binding activity. Cell 1991;64:573–84.
47. Somervaille TC, Linch DC, Khwaja A. Growth factor withdrawal from primary human erythroid progenitors induces apoptosis through a pathway involving glycogen synthase kinase-3 and Bax. Blood 2001;98:1374–81.
48. Bi Y, Stuelten CH, Kilts T, et al. Extracellular matrix proteoglycans control the fate of bone marrow stromal cells. J Biol Chem 2005;280:30481–9.
49. Steinbach JP, Weller M. Apoptosis in gliomas: molecular mechanisms and therapeutic implications. J Neurooncol 2004;70:245–54.